Improved virtual orbital multireference Møller–Plesset study of the ground and excited electronic states of protonated acetylene, $C_2H_3^+$

Rajat K. Chaudhuri[1,a)] and Karl F. Freed[2,b)]
[1]*Indian Institute of Astrophysics, Bangalore-560034, India*
[2]*The James Franck Institute and Department of Chemistry, University of Chicago, Chicago, Illinois 60637, USA*

The ground state geometries and associated normal mode frequencies of the classical and nonclassical protonated acetylene ion, i.e., the vinyl cation $C_2H_3^+$, are computed using the complete active space self-consistent field and improved virtual orbital (IVO) complete active space configuration interaction methods. In addition, the minimum-energy reaction path for the classical to nonclassical interconversion is determined (as are excitation energies) using the IVO modification of multireference Møller–Plesset (MRMP) perturbation theory. The IVO-MRMP treatment predicts the nonclassical structure to be 4.8 kcal/mol more stable than the classical one, which is consistent with other high level theoretical estimates. The proton affinity of acetylene from the IVO-MRMP treatment (154.8 kcal/mol) also agrees well with experiment (153.3 kcal/mol) and with earlier CASPT2 calculations (154.8 kcal/mol). We further report geometries and vibrational frequencies of low lying excited states of $C_2H_3^+$, which have not been observed and/or studied before. Comparisons with previous highly correlated calculations further demonstrate the computational efficiency of the IVO-MRPT methods. © *2008 American Institute of Physics.* [DOI: 10.1063/1.2958282]

I. INTRODUCTION

The vinyl cation $C_2H_3^+$ is of interest in many different areas of chemistry,[1–7] including astrochemistry.[8] *Ab initio* calculations[5] predict the vinyl cation as existing in two isomeric forms, a Y-shaped linear (classical) structure and a bridged (nonclassical) structure. Extensive theoretical and experimental studies to determine the relative stability of these two isomers conclude that the bridged shaped (nonclassical) structure is more stable than the Y-shaped (classical) one. Thus, the global minimum on the potential energy surface of $C_2H_3^+$ corresponds to the nonclassical structure. Although correlated *ab initio* many-body calculations[3,9–14] and infrared spectroscopic measurements[6,7] unambiguously favor the bridged structure as the more stable isomer, theoretical estimates of the energy difference between these two isomers range from 0.7 kcal/mol (Ref. 9) to 4.5 kcal/mol.[11]

Sharma *et al.*[15] and Psciuk *et al.*[14] summarize the normal mode frequencies of $C_2H_3^+$ isomers from computations using various *ab initio* many-body methods, including state-of-the-art coupled cluster calculations with singly and doubly excited clusters (CCSD). Second order perturbation theory[10,16] (MP2) predicts that the vibrational frequency for the lowest mode of classical structure is imaginary, i.e., that the Y-shaped linear structure is not a *stable* conformer. Likewise, several discrepancies exist between the theoretically predicted geometries.

While a plethora of information is available for the ground state of vinyl cation, including high quality estimates for its equilibrium geometry and vibrational frequencies, information regarding the excited state(s) is very limited. To our knowledge, only two vertical excitation energy calculations for this system are available using multireference configuration interaction with double excitations (MRD-CI) methods.[17,18] Moreover, these calculations assume a C_{2v} point group symmetry for the nonclassical structure instead of the correct C_s symmetry and, hence, are not very reliable.

In the present work, we compute the ground and excited state geometries of the $C_2H_3^+$ ion and the related spectroscopic constants. Vibrational frequencies of the ground and excited states are real, thereby supporting the reliability of the predicted geometries in contrast to prior treatments with imaginary frequencies. We also study the classical↔nonclassical minimum-energy reaction path as a function of the pseudointernal rotation angle. Calculations are also described for the potential energy curves (PECs) for both possible paths for the protonation of acetylene. The paths either involve protonation of the terminal carbon atom (producing the Y-shaped classical vinyl cation) or protonation of the center of the C—C bond (producing the bridged structure).

Section II briefly describes the theoretical methods applied here, while Sec. III summarizes the numerical results, presenting the geometries, normal mode frequencies, relative stabilities of the isomers, and transition energies. The PEC for protonation of acetylene and the nonclassical↔classical minimum-energy reaction path in the ground state are discussed in Sec. IV. Comparisons with MRCI and CC calculations further establish the computational efficiency of the IVO-MRPT methods used here for ground and excited states.

a)Electronic mail: rkchaudh@iiap.res.in.
b)Electronic mail: freed@uchicago.edu.

II. THEORY

The coupled cluster[19] (CC) formulation of the equation-of-motion[20,21] (EOM) method or the related linear response theory[22] (LRT) are widely used approaches for accurate electronic structure calculations. A great promise of these approaches arises because they *directly* evaluate energy differences and because the excitation energies scale properly in the noninteracting limit, so these methods are *size extensive*,[23] a crucial property for accurately determining state energies, bond cleavage energies, and related spectroscopic constants. Several applications exhibit the utility and strength of the EOM-CC/CCLRT method at the EOM-CCSD level (EOM coupled cluster theory with singles and double excitations). However, the use in CC schemes of a single determinantal reference function inhibits their application to bond breaking and curve crossing regions because these single reference approaches are incapable of providing accurate descriptions for states in quasidegenerate regions. Moreover, although the EOM-CCSD and its variants[24] are capable, in principle, of providing accurate estimates for transition energies and related properties, their computational expense limits their use to small molecular systems.

Multireference (MR) perturbation approaches, on the other hand, describe nondynamical electron correlation simply by using a small reference space containing reference functions that can adequately represent the quasidegeneracy, while dynamical electron correlation is introduced using MR-perturbation (MRPT) schemes. When applied to computing potential energy surfaces, some MRPT methods that are based on effective Hamiltonians are often plagued by ubiquitous intruder state problems,[25] thereby seriously limiting their viability for global potential surfaces. Among several recent attempts at devising a chemically accurate MRPT approach[26–32] for computing smooth potential surfaces, the most promising MRPT methods include those based on the use of a zeroth order multireference self-consistent field (MCSCF) or complete-active-space configuration interaction (CASCI) approximation, namely, the H^v,[26] MRMP,[27] MCQDPT,[28] CASPT2,[29] MRMP using APSG,[30] CIPSI,[31] etc., methods.

Recently, we have proposed a computationally inexpensive version of MRMP/MCQDPT in which the first order reference functions are generated from the improved virtual orbital complete active space configuration interaction (IVO-CASCI) method[33–37] and then are used in subsequent MR perturbation calculations. The IVO-CASCI scheme is computationally simpler than CI-singles (CIS) and complete active space SCF (CASSCF) methods. The latter arises because the IVO-CASCI calculations do not involve iterations beyond those in the initial SCF calculation, nor do they possess features that create convergence difficulties with increasing size of the CAS in CASCI calculations. Since the IVO-CASCI approach contains both singly and doubly excited configurations in the CAS (in addition to higher order excitations), it provides descriptions of both singly and doubly excited states with comparable accuracy to CASSCF treatments. The latter contrasts with the CIS method which cannot treat doubly excited states. Thus, the main computa-

TABLE I. Ground $^1A_1$ state geometry and vibrational frequencies of classical $C_2H_3^+$. Distances in Å, angles in deg, and frequencies in cm^{-1}. Entries within parentheses represent the number of contracted Gaussian orbitals (CGTO) used in the calculations.

	ACCD (73)	CCT (102)	ANO (136)	ACCT (161)
$R(C_2—H_3)$	1.080	1.071	1.071	1.071
$R(C_1—H_1)$	1.115	1.108	1.107	1.107
$R(C_1—C_2)$	1.281	1.269	1.268	1.268
$\angle H_1C_1C_2$ (α)	120.6	120.6	120.6	120.6
$\angle C_1C_2H_3$ (β)	180.0	180.0	180.0	180.0
$\angle H_1C_1H_2$ (γ)	118.8	118.8	118.8	118.8
ν_1	3429	3421	3423	3421
ν_2	3042	3022	3027	3022
ν_3	2957	2947	2951	2947
ν_4	1715	1713	1714	1713
ν_5	1168	1175	1178	1174
ν_6	1097	1125	1125	1125
ν_7	816	825	829	825
ν_8	206	477	499	476
ν_9	204	175	167	163

tional advantages of our new developed IVO-MCQDPT approach over the traditional MCQDPT method are (i) the absence of iterations beyond those in the initial SCF calculation and (ii) the lack of convergence difficulties from intruder states[25] that plague CASSCF calculations with increasing size of the CAS.

III. RESULTS AND DISCUSSION

The ground state electronic configurations of the classical and nonclassical vinyl cations are $[1-5]a_1(2)1b_1(2)1b_2(2)(X\ ^1A_1)$ and $[1-6]a'(2)a''(2) \times (X\ ^1A')$, respectively. The structural parameters for the ground and excited states of the vinyl cation are determined from CASSCF calculations with 10 active electrons and 12 active orbitals using the DALTON (Ref. 38) package, whereas the ground and excited state energies are computed using the IVO-CASCI formulation of the MCQDPT method (IVO-MCQDPT) that is now interfaced to GAMESS package.[39] Unless otherwise mentioned, no orbitals are frozen in these calculations.

A. Geometries

Because geometries and normal mode frequencies critically depend on the basis set, the reliability of our predicted geometries and normal mode frequencies is ensured by performing the CASSCF geometry optimization with basis sets of increasing size. Table I presents the structural parameters and vibrational frequencies for the ground $X\ ^1A_1$ state of classical $C_2H_3^+$ from $(10e, 12v)$ CASSCF calculations with aug-cc-pVDZ (Ref. 40) (ACCD), cc-pVTZ (Ref. 40) (CCT), atomic natural orbital[41] (ANO), and aug-cc-pVTZ (Ref. 40) (ACCT) basis sets. As observed from Table I, the C—H and C—C bond lengths decrease by 0.07 and 0.017 Å, respectively, when proceeding from the aug-cc-pVDZ to the aug-cc-pVTZ basis sets. Further improvement of the basis set to the ANO/aug-cc-pVTZ set merely alters the frequencies by a

TABLE II. Comparison of the ground state geometrical parameters of classical and nonclassical $C_2H_3^+$ obtained from the various *ab initio* many-body methods. Distances in Å and angles in deg.

Method	$R(CC)$	$R(C_1-H_1)$	$R(C_1-H_2)$	$R(C_2-H_3)$	α	β	γ
			Classical				
SCF[a]	1.263	1.086	1.086	1.075	119.9	180.0	120.2
SCF-CI[b]	1.275	1.098	1.098	1.087	120.3	180.0	119.4
CASSCF[c]	1.266	1.116	1.116	1.098	120.4	180.0	119.2
MP2	1.255	1.098	1.098	1.081	120.4	180.0	119.2
CCSD/6-311+G$(3df,2pd)$[d]	1.261	1.096	1.096	1.081	118.7	180.0	122.6
CASSCF	1.268	1.108	1.108	1.071	120.6	180.0	118.8
IVO-CASCI	1.268	1.095	1.095	1.095	120.7	180.0	118.6
			Nonclassical				
SCF[a]	1.210	1.276	1.073	1.073	61.7	179.1	119.2
SCF-CI[b]	1.234	1.281	1.084	1.084	61.7	179.1	118.6
CASSCF[c]	1.227	1.296	1.096	1.097	61.7	179.1	120.7
MP2	1.229	1.276	1.077	1.077	61.3	179.3	118.2
CCSD/6-311+G$(3df,2pd)$[d]	1.223	1.277	1.077	1.077	61.6	179.8	118.4
CASSCF	1.231	1.284	1.087	1.068	61.8	179.5	117.8
IVO-CASCI	1.240	1.311	1.088	1.088	61.8	179.6	117.9

[a]Reference 17.
[b]Reference 9.
[c]Reference 3.
[d]Reference 14.

few cm^{-1}, indicating that the computed bond lengths, bond angles, and the normal mode frequencies are fairly well converged with the CASSCF/CCT treatment. Nevertheless, all the calculations reported in subsequent tables are performed with the aug-cc-pVTZ basis for quality assurance.

Optimized ground state geometries of classical and nonclassical $C_2H_3^+$ from various *ab initio* many-body methods are presented in Table II for comparison. The present CASSCF calculations are performed with 161 contracted Gaussians (aug-cc-PVTZ), whereas Lindh *et al.*[3] use around 100 contracted Gaussian orbitals (CGTOs) (ANO). On the other hand, the CAS space used by Lindh *et al.* is much bigger than the present one. We further emphasize that the earlier CASSCF reports the structural parameters but not the normal mode frequencies which are equally relevant in judging their reliability.

As can be seen in Table II, the SCF geometry optimization for the nonclassical structure yields too short a C—C π bond to form a bridge structure. According to SCF calculations, the protonation of acetylene (giving rise to the nonclassical structure) increases the C—C bond by only 0.01 Å. The SCF-CI calculations estimate the C—C π bond for classical $C_2H_3^+$ to be 1.275 Å, whereas all other calculations except MP2 predict this C—C bond to be 1.26 Å. Moreover, MP2 calculations yield an imaginary-normal mode frequency for the classical structure (see Table III), which clearly indicates that MP2 optimized structure[10] for the classical $C_2H_3^+$ is not stable.

Table II exhibits some striking difference in the computed C—H bond lengths from various schemes, namely, (a) the present CASSCF calculations for the classical structure yield the C_2-H_3 bond as 0.037 Å shorter than the C_1-H_2 bond, whereas SCF,[17] SCF-CI,[9] CASSCF,[3] CCSD,[14] and MP2 calculations estimate the difference between these two bonds to be 0.011, 0.009, 0.018, 0.015, and 0.017 Å, respectively; (b) all calculations except the CASSCF/ACCT (the

present one) predict the C_2-H_3 and C_1-H_2 bond lengths to be equal, (c) the IVO-CASCI method estimates of the structural parameters for the nonclassical $C_2H_3^+$ ion are reasonably close to other theoretical values; however, the method predicts equal bond lengths for the C_2-H_3 and C_1-H_2 bonds of the classical structure. Table II further shows that the theoretically estimated C_1-H_1 bond length for the classical (nonclassical) $C_2H_3^+$ isomer varies from 1.086 Å (1.276 Å) to 1.116 Å (1.311 Å). Since experimental data (geometries) for these systems are not yet available, it is difficult to assess the accuracy of the theoretically computed quantities.

The present CASSCF calculations estimate the rotational constant for the rotation around the C≡C bond in nonclassical $C_2H_3^+$ to be 13.61 cm^{-1}, which compares well with the 13.41 cm^{-1} obtained by Lindh *et al.*[3] from CASSCF calculations.

It is also interesting to compare the ion geometries with that of acetylene to understand the changes occurring on protonation of acetylene. The CASSCF/aug-cc-pVTZ geometry optimization provides the C—C and C—H bonds of acetylene as 1.19 and 1.05 Å, respectively, close to the corresponding experimental values[42] of 1.20 and 1.06 Å. The numerical results presented in Table II indicate the following: (a) protonation of acetylene proceeds by weakening and lengthening of the C—C bond due to partial population of the π^* orbital; (b) the C—C bond length of acetylene is increased by 0.03 Å (0.06 Å) during protonation, producing the nonclassical (classical) structure; (c) the C_1-H_2 bonds (see Fig. 1) are increased by an equal amount (except for the $(10e, 12v)$ CASSCF calculations) during the perpendicular protonation of acetylene (as anticipated); and (d) the inclusion of electron correlation increases the C—H bond lengths.

TABLE III. The ground state vibrational frequencies (in cm^{-1}) for classical and nonclassical C$_2$H$_3^+$. Entries within parentheses are normal mode frequencies calculated from fitted potential energy surface.
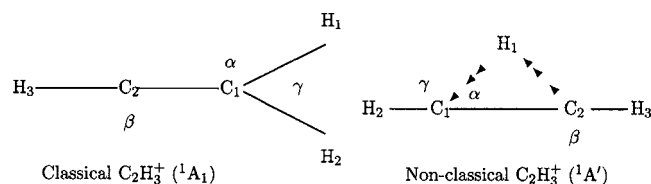
| | This work | | | | | |
	CASSCF	MP2	CCSD[a]	CCSD[b]	SCF+CI[c]	MP2[d]
			Classical			
ν_1	3421	3338	3280 (3328)	3303	3364	3327
ν_2	3022	3090	3073 (3084)	3115	3217	3103
ν_3	2947	3013	3009 (3017)	3040	3126	3028
ν_4	1713	1771	1724 (1730)	1745	1753	1783
ν_5	1174	1176	1176 (1159)	1206	1254	1161
ν_6	1125	1095	1078 (1077)	1092	1106	1097
ν_7	825	813	815 (801)	852	873	815
ν_8	476	673	614 (591)	633	601	686
ν_9	163	124	193 (199)	241	345	193i
			Nonclassical			
ν_1	3458	3396	3370 (3355)	3389	3443	3403
ν_2	3236	3289	3265 (3245)	3282	3339	3304
ν_3	2327	2402	2352 (2358)	2393	2471	2385
ν_4	1924	1926	1932 (1929)	1971	2000	1939
ν_5	1279	1324	1255 (1258)	1280	1279	1315
ν_6	935	913	908 (928)	926	923	917
ν_7	786	762	751 (775)	771	757	770
ν_8	718	700	580 (594)	621	513	696
ν_9	613	600	572 (534)	591	587	917

[a]Reference 15.
[b]Reference 14.
[c]Reference 9.
[d]Reference 10.

B. Normal mode frequencies

The normal mode frequencies for the ground state of classical and nonclassical C$_2$H$_3^+$ are compared with those published by Sharma et al.,[15] Psciuk et al.,[14] Lee et al.,[9] and by Lindh et al.[10] in Table III. The CCSD vibrational frequencies reported by Sharma et al. are obtained with the augmented aug-cc-pVTZ basis set, whereas Psciuk et al.[14] used CCSD/6-311+G(d,p) and CCSD/6-311+G($3df,2pd$) treatments. Lee et al. and Lindh et al., on the other hand, employ a double zeta plus polarization (DZ+P) basis for the CISD part and a TZ2Pf (triple zeta plus double polarization with an additional f function) basis for the MP2 calculation. Since the methods and basis sets differ between the calculations, the vibrational frequencies in Table III are not expected to be identical but should be similar.

Our MP2/aug-cc-pVTZ fundamental frequencies in Table III agree with those obtained from MP2/DZ+P calculation[10] to within 15 cm^{-1}, except for the lowest mode of the classical C$_2$H$_3^+$. However, this agreement is anticipated because both calculations use the same MP2 method and because our basis set comparison indicates that

both bases are sufficient. It is important to note that MP2/DZ+P,[10] MP2/6-311+G($2d,2p$),[16] MP2/6-311 +G(d,p), and MP2/6-311+G($3df,2pd$) (Ref. 14) calculations predict an imaginary frequency for mode ν_9, whereas all of our frequencies from MP2 calculations are real.

Table III further demonstrates the good agreement between the frequencies from the MP2/aug-cc-pVTZ and CCSD/aug-cc-pVTZ calculations, except for the lowest mode of classical C$_2$H$_3^+$. The frequencies from CASSCF/aug-

TABLE IV. Excited $^3A''$ state geometry and vibrational frequencies of C$_2$H$_3^+$. Distances in Å, angles in deg, and frequencies in cm^{-1}.

	CCT	ACCT
$R(C_2—H_3)$	1.075	1.097
$R(C_1—H_1)$	1.095	1.098
$R(C_1—H_2)$	1.101	1.076
$R(C_1—C_2)$	1.407	1.408
$\angle H_1C_1C_2$ (α)	121.0	121.1
$\angle C_1C_2H_3$ (β)	134.4	134.2
$\angle H_1C_1H_2$ (γ)	119.0	119.5
ν_1	3344	3329
ν_2	3135	3111
ν_3	3015	3079
ν_4	1485	1519
ν_5	1303	1305
ν_6	1125	1120
ν_7	1062	1096
ν_8	786	775
ν_9	785	775

FIG. 1. Geometrical structures of C$_2$H$_3^+$ ion.

TABLE V. Relative stability (in kcal/mol) of $C_2H_3^+$ isomers.

Method	$X\,^1A'$	$X\,^1A_1$
SCF	0.0	−3.7
MP2	0.0	8.7
CCSD	0.0	2.7
CASSCF	0.0	3.9
IVO-MRMP	0.0	4.8
MP2[a]	0.0	7.1
CEPA[b]	0.0	3.6
CCSD(T)[c]	0.0	3.66[d]

[a]Reference 16.
[b]Reference 3.
[c]Reference 14.
[d]cc-PVQZ basis set with CCSD/6-311+G($3pf,2pd$) optimized geometry.

cc-pVTZ calculations agree favorably with those from the CCSD/aug-cc-pVTZ and MP2/aug-cc-pVTZ treatments (except for ν_8, which is imaginary in two cases and quite different in one).

C. Relative stability and vertical excitation energies

Table V presents our calculations for the difference between the minimum energies of the classical and nonclassical isomers. It is evident from Table V that the inclusion of electron correlation (MP2 and IVO-MRPT) stabilizes the nonclassical structure with respect to the classical one. Several prior calculations exist for the stability of the nonclassical structure with respect to the classical isomer. For example, the coupled electron pair approximation (CEPA) calculations of Lischka and Köhler[13] predict the nonclassical structure to be 4.0 kcal/mol more stable than the classical one, and the MP2-R12 (MP2 with linear r_{12}-terms) calculations of Klopper and Kutzenligg[11] estimate this gap to be 4.5 kcal/mol. The MP2 and MP4 calculations of Lindh et al.[10] and Raghavachari et al.,[12] as well as very recent CCSD(T) calculations of Psciuk et al.,[14] also favor the bridged over the classical structure. The present estimate of the relative stability (4.8 kcal/mol) agrees well with most previous quantum mechanical calculations, except the MP2/aug-cc-pVTZ and MP2/6-311+G($2d,2f$) treatments that predict a much higher gap.

We have also computed the proton affinity of acetylene, i.e., the binding energy of the proton in the $C_2H_3^+$ ion, as 154.8 kcal/mol, which is in excellent agreement with experiment (153.3 kcal/mol) (Ref. 43) and with an earlier CEPA estimate of 154.8 kcal/mol by Lindh et al.[3]

The vertical excitation energies (VEEs) of C_2H_3 computed using the IVO-MCQDPT method are compared with the EOM-CCSD and MRD-CI (Ref. 18) approaches in Table VI. C_{2v} labels are used for convenience, but calculations for non-classical ion are made for C_s geometry of Table II. Vertical excitation energies of $C_sH_3^+$ have first been reported by Weber et al.[17] (SCF) and later by Gianturco and Schneider (MRDCI).[18] The VEEs from the IVO-MCQDPT method agree with the EOM-CCSD and MRD-CI (Ref. 18) treatments for both structures, but considerably less computer time is required. The $X\,^1A'$-$1\,^3A''$ adiabatic transition energy

TABLE VI. Vertical excitation energies (in eV) of classical and nonclassical $C_2H_3^+$. (Adiabatic excitation energy is given within parentheses.)

State	IVO-MCQDPT	Classical		MRD-CI[b]
		EOM-CCSD	MRD-CI[a]	
		Classical		
$1\,^3A_2$	2.56	2.57		
$1\,^1A_2$	3.11	3.22	2.37	3.22
$1\,^3A_1$	5.40	5.48		
$1\,^1A_1$	6.45	7.60	6.95	7.40
$1\,^3B_2$	7.10	7.44		
$1\,^1B_2$	7.87	8.36		
		Nonclassical		
$1\,^3A'$	6.09	6.12		
$1\,^3A''$	6.16	6.30		
	(2.10)	(2.16)		
$1\,^1A''$	6.76	6.94	6.53	7.01
$1\,^1A'$	8.36	9.02	11.36	9.14

[a]Reference 17.
[b]Reference 18.

is provided in parentheses, and the optimized geometry and normal mode frequencies for the $1\,^3A''$ excited state of the nonclassical isomer are given in Table IV.

IV. POTENTIAL ENERGY CURVES

Escribano and Bunker[44] have proposed a pseudointernal rotation angle ρ that serves to interconvert between the minima for the two isomeric structures. Sharma et al. and Psciuk et al. employed this reaction path in their calculations of the PEC for the interconversion. We also use the reaction path, but for simplicity the geometry is not optimized for each pseudointernal rotation angle ρ. Figure 2 depicts the PEC for the minimum-energy reaction path for the nonclassical↔classical $C_2H_3^+$ interconversion as a function
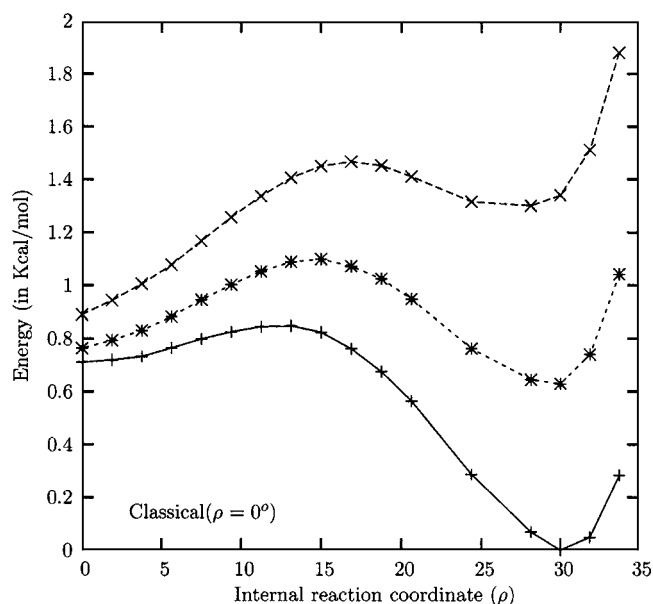

FIG. 2. Plot of classical↔nonclassical reaction path. In this figure, symbols +, *, and × correspond to $R(C_1—H_1)$=1.104, 1.094, and 1.084 Å, respectively.
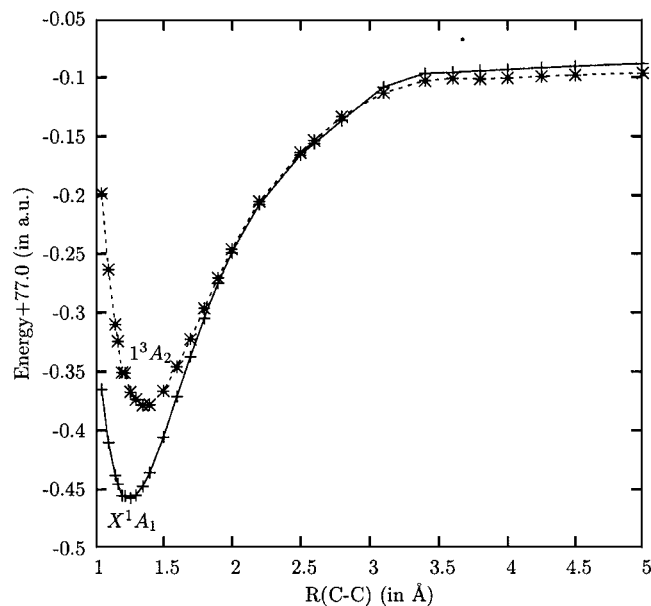
FIG. 3. Plot of ground $X\,^1A_1$ and excited $^3A_2$ state potential energy curves of classical $C_2H_3^+$ as a function of $R(C-C)$. All other parameters are fixed at their aug-cc-pVTZ optimized values.
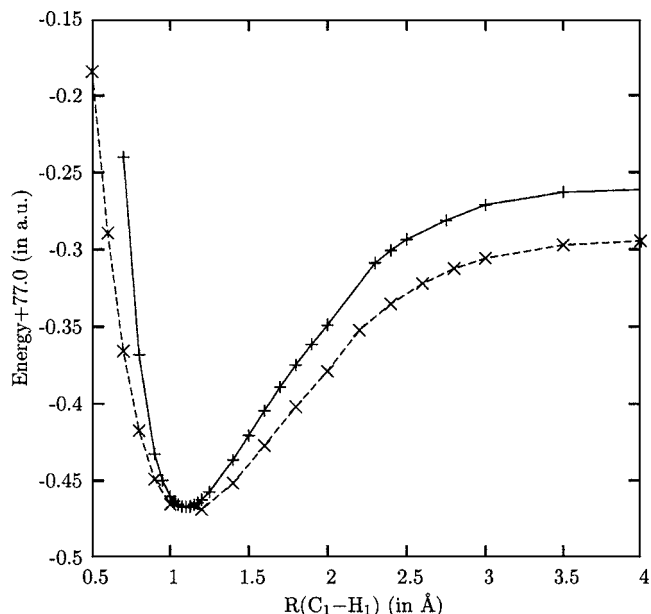

FIG. 4. Plot of ground state potential energy curve of classical $C_2H_3^+$ as a function of $R(C_1-H_1)$ with $R(C=C)=1.268$ Å and $R(C-H)=1.071$ Å. In this figure, symbols x and $+$ correspond to perpendicular (nonclassical type) and lateral/terminal protonation of C_2H_2.

of pseudointernal rotation angle ρ, where $\rho=0$ corresponds to the classical structure and $\rho=30$ to the nonclassical isomer. The figure also presents the PEC obtained for two different values of $R(C_1-H_1)$. Figure 2 exhibits the potential energy as reaching a global minimum at $\rho=30$ for $R(C_1H_1)$ $=1.104$ Å. However, as the C_1-H_2 bond increases to 1.094 Å, both the nonclassical and classical structures become equally stable, and for $R(C_1H_1)=1.084$ Å, the classical structure becomes the most stable isotope. Although we have not optimized the geometry for each ρ, the figure still demonstrates the qualitatively correct picture. The present estimate ~ 0.4 kcal/mol of the barrier height (with respect to the classical geometry) along the reaction path agrees fairly well with CEPA calculations of Lindh et al.[3] but deviates by ± 0.3 kcal/mol from MRCI (Ref. 3) (0.7 kcal/mol) and CCSD (Ref. 14) (0.11 kcal/mol) values.

Figure 3 presents the ground $X\,^1A_1$ and excited $^3A_2$ states PECs for the classical $C_2H_3^+$ ion as a function the $C=C$ distance. The ground $X\,^1A_1$ and excited $^3A_2$ states of the $C_2H_3^+$ ion cross near $R(C-C)-2.0$ Å. Figure 3 further shows that the excited $^3A_2$ state has a minimum at $R=1.40$ Å, which agrees with our CASSCF geometry optimization for the $^3A_2$ state (see Table IV).

Figure 4 depicts the PEC curves for the protonation of acetylene along a perpendicular path to the nonclassical isomer and along a lateral path to the classical structure. The greater stability of the bridged structure (nonclassical) than the classical one is reflected in the PECs for the protonation of acetylene as function of the acetylene-H^+ separation where the dissociation energy for nonclassical $C_2H_3^+$ is less than that required for the classical structure.

V. CONCLUDING REMARKS

Theoretical calculations using the CASSCF and our recently proposed IVO-CASCI based MRMP/MCQDPT method provide the following conclusions.

(a) The CASSCF optimized geometrical parameters and normal mode frequencies of the vinyl cation agree fairly well with previous high level theoretical values. The calculation further supports the predicted existence of a stable excited state of the vinyl cation.

(b) The geometries obtained from the computationally inexpensive IVO-CASCI procedure agree well with available theoretical data.

(c) The relative stability and proton affinity determined from IVO-MRMP and CCSD calculations accord well with earlier calculations, and our computed proton affinity for acetylene (154.8 kcal/mol) is in agreement with the experiment value of 153.3 kcal/mol.

(d) The low lying vertical excitation energies from the IVO-MCQDPT treatment are in accord with the state-of-the-art CCSD and previous high level theory.

(e) The present calculations further demonstrate that the IVO-MRMP method is capable of providing reliable energies even for complicated systems. We further emphasize that IVO-CASCI and IVO-MRMP/MCQDPT methods are highly cost effective compared to other sophisticated electronic structure theories. The IVO-CASCI (numerical derivative) geometry optimization takes only $\frac{3}{4}$ of the time that required for CASSCF geometry optimization, and significant additional speed enhancement will accrue from analytical derivative methods under development.

(f) The present study reports the geometries and vibrational frequencies for the low lying excited state of $C_2H_3^+$, which to our knowledge have not been studied or observed before. However, the favorable agreement of our predicted geometries and spectroscopic constants for ground states of $C_2H_3^+$ with highly correlated theoretical data suggest that the our computed spectro-

scopic constants for this system should be equally reliable.

(g) We emphasize that the IVO-MRMP/MCQDPT is computationally much less expensive than the MCSCF based MRMP/MCQDPT and CCSD methods.

ACKNOWLEDGMENTS

[1] R. K. Janev and D. Reiter, Phys. Plasmas **9**, 4071 (2002); Contrib. Plasma Phys. **43**, 401 (2003); J. Nucl. Mater. **313**, 1202 (2003); Phys. Plasmas **11**, 780 (2004).

[2] D. Marx and M. Parrinello, Science **271**, 179 (1996).

[3] R. Lindh, B. O. Roos, and W. P. Kraemer, Chem. Phys. Lett. **139**, 408 (1987).

[4] C. Liang, T. P. Hamilton, and H. F. Schaefer III, J. Chem. Phys. **92**, 3653 (1990).

[5] B. Zurawski, R. Alrichs, and W. Kutzelnigg, Chem. Phys. Lett. **21**, 309 (1973).

[6] M. W. Crofton, M. F. Jagod, B. D. Rehfuss, and T. Oka, J. Chem. Phys. **91**, 5139 (1989).

[7] C. M. Gabrys, D. Uy, M. F. Jagod, T. Oka, and T. Amano, J. Am. Chem. Soc. **90**, 15611 (1995).

[8] A. E. Glassgold, A. Omont, and M. Guelin, Astrophys. J. **396**, 115 (1992).

[9] T. J. Lee and H. F. Schaefer III, J. Chem. Phys. **84**, 3437 (1986).

[10] R. Lindh, J. E. Rice, and T. J. Lee, J. Chem. Phys. **94**, 8008 (1991).

[11] W. Klopper and W. Kutzelnigg, J. Phys. Chem. **94**, 5625 (1990).

[12] K. Raghavachari, R. A. Whiteside, J. A. Pople, and P. v. R. Schleyer, J. Am. Chem. Soc. **105**, 5649 (1981).

[13] H. Lischka and H. J. Köhler, J. Am. Chem. Soc. **100**, 5297 (1978).

[14] B. T. Psciuk, V. A. Benderskii, and H. B. Schlegel, Theor. Chem. Acc. **118**, 75 (2007).

[15] A. R. Sharma, J. Wu, B. J. Braams, S. Carter, R. Shneider, B. Shepler, and J. W. Bowman, J. Chem. Phys. **125**, 224306 (2006).

[16] G. E. Douberly, A. M. Ricks, B. W. Ticknor, W. C. McKee, P. v. R. Schleyer, and M. A. Duncan, J. Phys. Chem. A **112**, 1897 (2008).

[17] J. Weber, M. Yashimine, and A. D. Mclean, J. Chem. Phys. **64**, 4159 (1976).

[18] F. A. Gianturco and F. Schnider, J. Chem. Phys. **95**, 7965 (1991).

[19] F. Coester, Nucl. Phys. **7**, 421 (1958); F. Coester and H. Kümmel, Nucl. Phys. **17**, 477 (1960); J. Čížek, J. Chem. Phys. **45**, 4256 (1966); Adv. Chem. Phys. **14**, 35 (1969); J. Čížek and J. Paldus, Adv. Chem. Phys. **9**, 105 (1975); R. J. Bartlett and W. D. Silver, Int. J. Quantum Chem. **S9**, 183 (1975); R. J. Bartlett, J. Phys. Chem. **93**, 1697 (1989); in *Modern Electronic Structure Theory*, edited by D. R. Yarkony (World Scientific, Singapore, 1995).

[20] H. Sekino and R. J. Bartlett, Int. J. Quantum Chem. **S18**, 255 (1984); J. F. Stanton and R. J. Bartlett, J. Chem. Phys. **98**, 7029 (1993).

[21] M. F. Herman, K. F. Freed, and D. L. Yeager, Adv. Chem. Phys. **48**, 1 (1981).

[22] H. J. Monkhorst, Int. J. Quantum Chem. **S11**, 421 (1977); D. Mukherjee and P. K. Mukherjee, Chem. Phys. **39**, 325 (1979); S. Ghosh, D. Mukherjee, and S. N. Bhattacharyya, Chem. Phys. **72**, 1611 (1982); S. Ghosh, D. Mukherjee, and S. N. Bhattacharyya, Mol. Phys. **43**, 173 (1981).

[23] R. J. Bartlett, Annu. Rev. Phys. Chem. **32**, 359 (1981).

[24] J. D. Watts and R. J. Bartlett, J. Chem. Phys. **101**, 3073 (1994); Chem. Phys. Lett. **233**, 81 (1995).

[25] T. H. Schucan and H. A. Weidenmüller, Ann. Phys. **73**, 108 (1972).

[26] K. F. Freed, in *Lecture Notes in Chemistry*, edited by U. Kaldor (Springer-Verlag, Berlin, 1989), Vol. 52.

[27] K. Hirao, Int. J. Quantum Chem. **S26**, 517 (1992); Chem. Phys. Lett. **201**, 59 (1993).

[28] H. Nakano, J. Chem. Phys. **99**, 7983 (1993).

[29] K. Andersson, P. Å. Malmqvist, B. O. Roos, A. J. Sadlej, K. Wolinski, J. Phys. Chem. **94**, 5483 (1990); K. Andersson, P. Å. Malmqvist, and B. O. Roos, J. Chem. Phys. **96**, 1218 (1992).

[30] E. Rosta and P. R. Surján, J. Chem. Phys. **116**, 878 (2002); P. R. Surján, Z. Rolik, A. Szabados, and D. Köhalmi, Ann. Phys. **13**, 223 (2004).

[31] B. Huron, J. P. Malrieu, and P. Rancurel, J. Chem. Phys. **58**, 5745 (1973); R. Cimiraglia, *ibid.* **83**, 1746 (1985).

[32] U. S. Mahapatra, B. Datta, and D. Mukherjee, J. Phys. Chem. A **103**, 1822 (1999); P. Ghosh, S. Chattopadhyay, D. Jana, and D. Mukherjee, Int. J. Mol. Sci. **3**, 733 (2002).

[33] D. M. Potts, C. M. Taylor, R. K. Chaudhuri, and K. F. Freed, J. Chem. Phys. **114**, 2592 (2001).

[34] R. K. Chaudhuri, K. F. Freed, and D. M. Potts, in *Low lying Potential energy surfaces*, edited by M. R. Hoffman and K. G. Dyall (Oxford University, Press, New York, 2002), Vol. 828, p. 154; R. K. Chaudhuri, K. F. Freed, S. A. Abrash, and D. M. Potts, J. Mol. Struct.: THEOCHEM **83**, 547 (2001).

[35] C. M. Taylor, R. K. Chaudhuri, and K. F. Freed, J. Chem. Phys. **122**, 044317 (2005).

[36] R. K. Chaudhuri and K. F. Freed, J. Chem. Phys. **122**, 204111 (2005), and references therein.

[37] R. K. Chaudhuri, K. F. Freed, and U. S. Mahapatra, J. Chem. Phys. **128**, 144304 (2008); R. K. Chaudhuri and S. L. N. G. Krishnamachari, J. Phys. Chem. A **112**, 4399 (2008).

[38] Release 1.2 (2001), written by T. Helgaker, H. J. Aa. Jensen, P. Joergensen, *et al.*.

[39] M. W. Schmidt, K. K. Baldridge, J. A. Boatz, S. T. Elbert, M. S. Gordon, J. H. Jensen, S. Koseki, N. Matsunaga, K. A. Nguyen, S. J. Su, T. L. Windus, M. Dupuis, and J. A. Montgomery, J. Comput. Chem. **14**, 1347 (1993).

[40] T. H. Dunning, J. Chem. Phys. **53**, 2823 (1970); **55**, 716 (1971).

[41] P. O. Widmark, P. A. Malmqvist, and B. O. Roos, Theor. Chim. Acta **77**, 291 (1990).

[42] G. Herzberg, *Molecular Spectra and Molecular Structure*, Electronic Spectra and Electronic Structure of Polyatomic Molecules (Von Nostrand Reinhold Company, New York, 1966).

[43] S. G. Lias and F. J. Liebman, J. Phys. Chem. Ref. Data **13**, 695 (1984).

[44] R. Escribano and P. R. Bunker, J. Mol. Spectrosc. **122**, 325 (1987).